NJC

ROYAL SOCIETY OF CHEMISTRY

PAPER

View Article Online
View Journal | View Issue

Check for updates

Cite this: *New J. Chem.*, 2020, 44, 20823

Refining the model to design α-chymotrypsin superactivators: the role of the binding mode of quaternary ammonium salts†

Francesco Gabriele,[a] Laura Goracci,*[b] Raimondo Germani[b] and Nicoletta Spreti*[a]

Received 21st September 2020,
Accepted 9th November 2020

DOI: 10.1039/d0nj04676k

rsc.li/njc

A number of quaternary ammonium salts with bulky hydrophobic moieties are known to provoke the superactivation of α-chymotrypsin (α-CT) in aqueous solution. In particular, benzyl-substituted ammonium and dicationic ammonium-based salts have recently emerged as promising classes of compounds to induce α-CT superactivation and stabilization. Preliminary *in silico* modelling suggested the α-CT residue tryptophan 215 to be the major anchor point of these additives. In order to achieve a broader knowledge of the enzyme–additive interactions and to validate the modelling studies, new ammonium-based additives were designed and tested. The hydrophobic interaction resulted in being critical to improving superactivation, with [(2,3,5,6-tetramethyl-*p*-phenylene)dimethylene]bis[triethylammonium bromide] (bisEDuEAB) resulting as the most effective quaternary ammonium superactivating agent studied so far. Finally, a general agreement between *in silico* outcomes and kinetic parameters was observed, and data interpretation is discussed based on the proposed α-CT/additive binding modes.

1. Introduction

α-Chymotrypsin (α-CT) (EC 3.4.21.1), a hydrophilic globular serine protease, represents one of the most studied model enzymes, and its structure and mechanism of action are well-known since the 1970s.[1–3] For this reason, the effect of additives and new reaction media on the enzyme catalytic properties has been extensively studied and reviewed. Many studies in the literature have been devoted to the superactivating effect of hydrophilic additives on α-CT, such as cationic single-chain[4–6] and gemini surfactants[7–9] and polyamines.[10] The enhancement of enzyme catalytic activity induced by these additives has been attributed to hydrophobic interactions between the additives and the protein and this effect was mainly due to an increase of the enzyme catalytic activity.

Polyelectrolytes are also able to induce α-CT superactivation,[11,12] modifying the electrostatic fields around the enzyme. The favorable interactions between enzyme and substrate led to an increase in both affinity (K_M) and catalytic constant (k_{cat}). In particular, kosmotropes were able to stabilize the tertiary structure of the enzyme and to increase hydrophobic interactions between the enzyme and the substrate.

Recently, the effect of co-solvents, stabilizers, pressure and temperature on the α-CT hydrolysis of the peptide bond was also investigated.[13–15]

For many years our research group has been studying the effect of hydrophilic additives on the activity and stability of α-CT; the enzyme was proved to be superactivated by a number of cationic surfactants and a bulky hydrophobic head group seemed to play a decisive role.[16,17] In fact, in the presence of cetyltributylammonium bromide (CTBABr), the instantaneous activity of the enzyme increased by 8 times compared to that of the buffer. However, further studies indicated that the amphiphilic nature of the additives was not essential, since ammoniums salts, like tetrabutylammonium bromide (TBABr), which possesses the same head group of CTBABr but lacks the long hydrocarbon chain, led to the same significant superactivation (*i.e.* 8-fold increase of instantaneous activity) and, in addition, enzyme superactivation is maintained for over two months.[18]

The effect produced by the "big head" additives on the activity of α-CT with natural substrates was also assessed using electron spray ionization mass spectrometry (ESI-MS)[19] and with model substrates containing more amino acid residues than the model substrate, *N*-glutaryl-L-phenylalanine *p*-nitroanilide (GPNA) used in previous studies.[20]

The activation effect of the "big head" additives was rationalized by assuming that the proximity of the additive to the

[a] *Department of Physical and Chemical Sciences, University of L'Aquila, Via Vetoio, I-67100 Coppito, L'Aquila, Italy*
[b] *Department of Chemistry, Biology and Biotechnology, University of Perugia, via Elce di Sotto 8, I-06123, Perugia, Italy. E-mail: laura.goracci@unipg.it*

† Electronic supplementary information (ESI) available. See DOI: 10.1039/d0nj04676k

active site led to an increase in its hydrophobicity and therefore to a greater nucleophilicity of the serine 195 (S195) hydroxyl group, which was mainly responsible for the enzymatic activity.

More recently, cationic ammonium-based additives bearing a benzylic group were synthesized and tested.[21] In particular, the effect of benzyltrimethylammonium bromide (BzTMABr), benzyltributylammonium bromide (BzTBABr) and benzyldodecyldimethylammonium bromide (BzDDABr) was investigated. A significant increase in the GPNA hydrolysis instantaneous rate was observed, with a greater effect of BzTBABr. However, this effect was accompanied by a faster deactivation of the enzyme compared to pure buffer.

In addition to the benzyl-substituted ammonium salt, two novel dicationic salts, (1,8-bis(tributylammonium)octane dibromide (bisBOAB) and 1,4-bis(tributylammonium)xylene dibromide (bisBAB)) were also synthesized and tested.[21] The major difference between the two dicationic salts was in the linker moiety, which was flexible and rigid, respectively. bisBOAB, which can be considered as a dimer of TBABr, induced similar superactivation and stabilization effects when compared to the monomer, but at a lower concentration. In the case of the more rigid bisBAB, the superactivation effect was reduced compared to the more flexible bisBOAB and enzyme deactivation was faster.

The collected data were used to perform molecular modelling studies aiming at rationalizing the observed kinetic effects. The proposed *in silico* model[21] suggested that the residue tryptophan 215 (W215), which is located adjacent to the catalytic site, may represent the anchor point for the quaternary ammonium salts possessing a superactivation effect. More precisely, small size quaternary ammonium-based additives with reduced flexibility (*e.g.* BzTBABr) were proposed to interact with W215. Due to this binding mode, an increase in the hydrophobicity of the catalytic site occurs, with a consequent increase in the k_{cat} value. For dicationic ammonium salts, the greater flexibility of the spacer in bisBOAB induced alternative binding modes for the alkyl chains, while the rigid structure for bisBAB seemed to be not optimized to simultaneously interact with W215 and with the hydrophobic region generated by histidine 57 (H57). Therefore, the binding poses for dicationic ammonium salts were in agreement with the lower superactivation effect. These modelling studies and experimental evidences suggested that enzyme catalytic properties could be strongly influenced not only by a number of structural features of the additive (*i.e.* charge, charge density, size, and hydrophobic/hydrophilic balance), but also by specific additive/enzyme interactions.

This work aimed at validating the previously generated hypotheses and the proposed *in silico* model for the interaction between ammonium-based additives and α-CT. To this aim, novel ammonium-based additives were designed, synthesized and tested to validate the hypothesized binding mode. The effect of additives on α-CT catalyzed hydrolysis of GPNA was studied and the determination of kinetic parameters allowed us to better understand the reasons for enzyme superactivation and to estimate the predictive capacity of the model used.

2. Experimental

2.1 Materials

Crystalline bovine pancreatic α-chymotrypsin (EC 3.4.21.1) (α-CT, 24.8 kDa, type II: 3 times crystallized, dialyzed and lyophilized), *N*-glutaryl-L-phenylalanine-*p*-nitroanilide (GPNA), Tris used for buffer preparation and *p*-nitroaniline used for molar absorption coefficient determination were purchased from Sigma-Aldrich (St. Louis MO, USA). Buffered solutions of enzyme and substrate were freshly prepared immediately before use. All chemicals and solvents, all of analytical grade, were purchased from Merck, and were used as received without further treatment.

2.2 Synthesis of additives

Mono- and dicationic quaternary ammonium salts were synthesized by the quaternization of the respective tertiary amines with the appropriate bromo derivatives. Melting points were determined on the Barloworld Scientific Stewart SMP3 apparatus and are uncorrected. ^{1}H-NMR spectra were registered on a Bruker AVANCE DRX 400 instrument using $CDCl_3$, CD_3OD or D_2O as solvents at 25.0 °C. Chemical shifts are given in ppm relative to the residual ^{1}H solvent signal.

Trimethyl(3-phenylpropyl)ammonium bromide (PhPrTMABr) was obtained by reaction of (3-bromopropyl)benzene (50 mmol) with trimethylamine (molar ratio 1 : 1.5) in EtOH, under magnetic stirring for 12 h at room temperature. After the removal of the solvent, the solid was purified by crystallization. Yield 12.1 g, 94%, m.p. 150–152 °C (ethyl acetate-methanol). δH (400 MHz, CD_3OD) 2.10–2.18 (2H, m, CH_2), 2.73 (2H, t, CH_2), 3.12 (9H, s, $N^+(CH_3)_3$), 3.33–3.38 (2H, m, Ph-CH_2); 7.33–7.20 (5H, m, Ph).[22]

Tributyl(3-phenylpropyl)ammonium bromide (PhPrTBABr) was obtained starting from (3-bromopropyl)benzene (50 mmol) *via* reaction with tributylamine (molar ratio 1 : 1.5) in CH_3CN; the mixture was refluxed for 3 days. The reaction raw product after elimination of the solvent was taken up with ethyl ether until a solid was obtained; the latter was purified by double crystallization from a mixture of ethyl acetate/ethyl ether. Yield 13.8, 72%, m.p. 79–81 °C (ethyl acetate–ethyl ether). δH (400 MHz, CD_3OD) 0.99 (9H, t, $3CH_3$), 1.36 (6H, m, $3CH_2$), 1.53 (6H, m, $3CH_2$), 2.10 (2H, m, Ph-CH_2-CMx0048;$_{12}$-), 2.73 (2H, t, Ph-CH_2), 3.21 (8H, m, $4CH_2$), 7.39–7.17 (5H, m, Ph).

Hexamethylene bis(triethylammonium)dibromide (bisEHAB) was synthesized by quaternization of 1,6-dibromohexane (41 mmol) with triethyl amine (molar ratio 1 : 2.1) in CH_3CN; the mixture was refluxed under magnetic stirring for 8 h. After removal of the solvent, the solid was purified by crystallization from an acetone/ethyl ether mixture. Yield 14.1 g, 75%, m.p. 267–268 °C decompn (acetone–ethy lether).

δH (400 MHz, CD_3OD) 1.36 (18H, t, $6CH_3$), 1.55 (4H, m, $2CH_2$), 1.84 (4H, m, $2CH_2$), 3.24 (4H, m, $2CH_2$). 3.40 (m, 12H, $6CH_2$).[23]

Hexamethylene bis(tributylammonium)dibromide (bisBHAB) was prepared by quaternization of 1,6-dibromohexane (41 mmol) with tributylamine (molar ratio 1 : 2.2) in acetonitrile; the mixture was refluxed under magnetic stirring for 6 days. After removal of

the solvent, the solid was purified by several times crystallization from an acetone/ethyl ether mixture. Yield 8.8 g, 50%, m.p. 168–170 °C decompn. (acetone–ethyl ether).

δH (400 MHz, D_2O) 0.95 (18H, t, $6CH_3$), 1.37 (16H, m, $8CH_2$), 1.66 (16H, m, $8CH_2$), 3.21 (16H, m, 8 CH_2).[24]

BisEDuEAB and bisEOMeEAB were obtained from durene and 1,4-dimethoxybenzene respectively. These compounds were initially converted into dibromo derivatives with formaldehyde and hydrobromic acid by reflux into acetic acid, according to the procedure described in the literature.[25]

1,4-Bis(bromomethyl)-2,3,5,6-tetramethylbenzene, purified by crystallization, m.p. 216–218 °C (ethyl acetate), yield 96%. δH (400 MHz, $CDCl_3$) 2.33 (12H, s, $4CH_3$), 4.60 (4H, s, $2CH_2$).

1,4-Bis(bromomethyl)-2,5-dimethoxybenzene, purified by crystallization, m.p. 202–203 °C (methanol), yield 86%. δH (400 MHz, $CDCl_3$) 3.87 (6H, s, $2OCH_3$), 4.53 (4H, s, $2CH_2$), 6.86 (s, 2H, Ph).

[(2,3,5,6-Tetramethyl-*p*-phenylene)dimethylene] bis[triethylammonium bromide] (bisEDuEAB) was synthesized by reaction of 1,4-bis(bromomethyl)-2,3,5,6-tetramethylbenzene (32 mmol) with triethylamine (molar ratio 1 : 2.1) in CH_3CN; the mixture was refluxed for 6 h. Purified by double crystallization from an acetone-methanol mixture. Yield 11.5 g, 88%, m.p. 206–208 °C decompn.

δH (400 MHz, D_2O) 1.23 (18H, s, $6CH_3$), 2.44 (12H, s, $4CH_3$), 3.34 (12H, m, $6CH_2$); 4.89 (4H, s, $2CH_2$).

[(2,5-Dimethoxy-*p*-phenylene)dimethylene]bis[triethylammonium bromide] bisEOMeEAB was synthesized by reaction of 1,4-bis-(bromomethyl)-2,5-dimethoxybenzene (31 mmol) with triethylamine (molar ratio 1 : 2.1) in acetonitrile; the mixture was refluxed under magnetic stirring for 10 h. Purified by double crystallization. Yield 9.8g, 75%, m.p. 218–220 °C (acetone–methanol).

δH (400 MHz, CD_3OD) 1.46 (18H, t, $6CH_3$), 3.48–3.29 (12H, m, $6CH_2$), 3.98 (6H, s, $2OCH_3$), 4.57 (4H, s, Ph–CH_2–N), 7.30 (2H, s, Ph).[26]

2.2 α-Chymotrypsin activity assay

The α-CT activity assay was already described elsewhere.[21] Briefly, α-CT activity was measured spectrophotometrically at 25.0 ± 0.1 °C, monitoring the increase in absorbance at 410 nm related to *p*-nitroaniline (*p*NA), the hydrolysis product of GPNA. The molar absorption coefficient (ε_{410}) of *p*NA is 8800 M^{-1} cm^{-1} in pure buffer. Absorbance variation in the presence of the additives at the tested concentrations was evaluated and used in rate value estimations. A Shimadzu UV-160A UV-VIS spectrophotometer equipped with a thermostated cell was used in this study. The α-CT activity assay mixture was prepared in 0.1 M Tris–HCl buffer at pH 7.75, with an enzyme concentration of 0.2 mg ml^{-1} (8 μM) and a concentration of the substrate GPNA of 2.5×10^{-3} M. The pH of the mixture remained constant during analysis. The linear increase of absorbance at 410 nm due to *p*NA formation was recorded as a function of time for 300 seconds. Concerning the parameters discussed in this study, the reaction rate of α-CT (*i.e.* moles of *p*NA formed per unit of time) was calculated from the slope of the initial linear curve of *p*NA concentration *vs.* time. The kinetic parameters k_{cat} and K_m in pure buffer and in the presence of additives were derived by linear regression analysis of the double reciprocal Lineweaver–Burk plots in a range of substrate concentration between 0.1×10^{-3} M and 2.5×10^{-3} M. Experiments were reproduced at least three times and the differences between duplicates in each experiment were always below 5%.

2.3 Molecular modelling studies

The possible binding poses of the tested additives in the surroundings of the α-CT catalytic site were explored using the FLAP (Fingerprints for Ligands and Proteins) software (Molecular Discovery Ltd, UK).[27] The docking procedure to study the α-CT/additive interaction is described elsewhere.[21] Briefly, the X-ray α-CT structure (pdb code: 4CHA) was processed in FLAP to describe the catalytic cavity in terms of the GRID Molecular Interaction Fields (MIFs).[28,29] Probes used to generate the MIFs were H (shape), DRY (hydrophobic interactions), N1 (H-bond donor) and O (H-bond acceptor) interactions. Thus, the binding poses of the additives in the α-CT cavity were generated using FLAP in the structure-based mode,[30–32] with 50 conformations for each additive considered. The 10 top-ranked poses according to the Glob-Prod descriptor for each additive were visually inspected. The same approach was used in this study to predict the most probable binding mode of GPNA into the α-CT cavity.

3. Results and discussion

3.1 General design approach

The design of novel ammonium-based additives was performed based on a molecular modelling approach previously described.[21] Briefly, in that study the FLAP software was used to evaluate the most probable binding pose of four ammonium based additives, aiming at identifying the molecular interactions potentially responsible for the catalytic effect. The four tested additives represented three scaffolds (Fig. 1): (a) aromatic substituted quaternary ammonium additives (BzTMABr, BzTBABr); (b) diammonium-based additives with a flexible linker (bisBOAB); and (c) diammonium-based additives with a rigid linker (bisBAB). Here, the previously generated models for each additive were used as a starting point for the rational design of new analogues, aiming not only at optimizing the catalytic effect, but also at validating the hypothesis previously generated. Using the FLAP editing tool, two new additives for each scaffold were designed, in the attempt to optimize their interaction with the α-CT cavity (pdb code: 4CHA) in terms of the maximum overlap of GRID molecular interaction fields (see the Methods section for details). The structure of the new additives is also shown in Fig. 1. The design and the observed catalytic effect for each scaffold is separately discussed in the next paragraphs.

3.2 Design of phenyl-based ammonium additives and their effect on α-CT activity

Concerning the phenyl-based ammonium additives (Fig. 1-a), previous studies demonstrated a superactivating effect of benzyl-substituted ammonium salts, especially BzTBABr, and

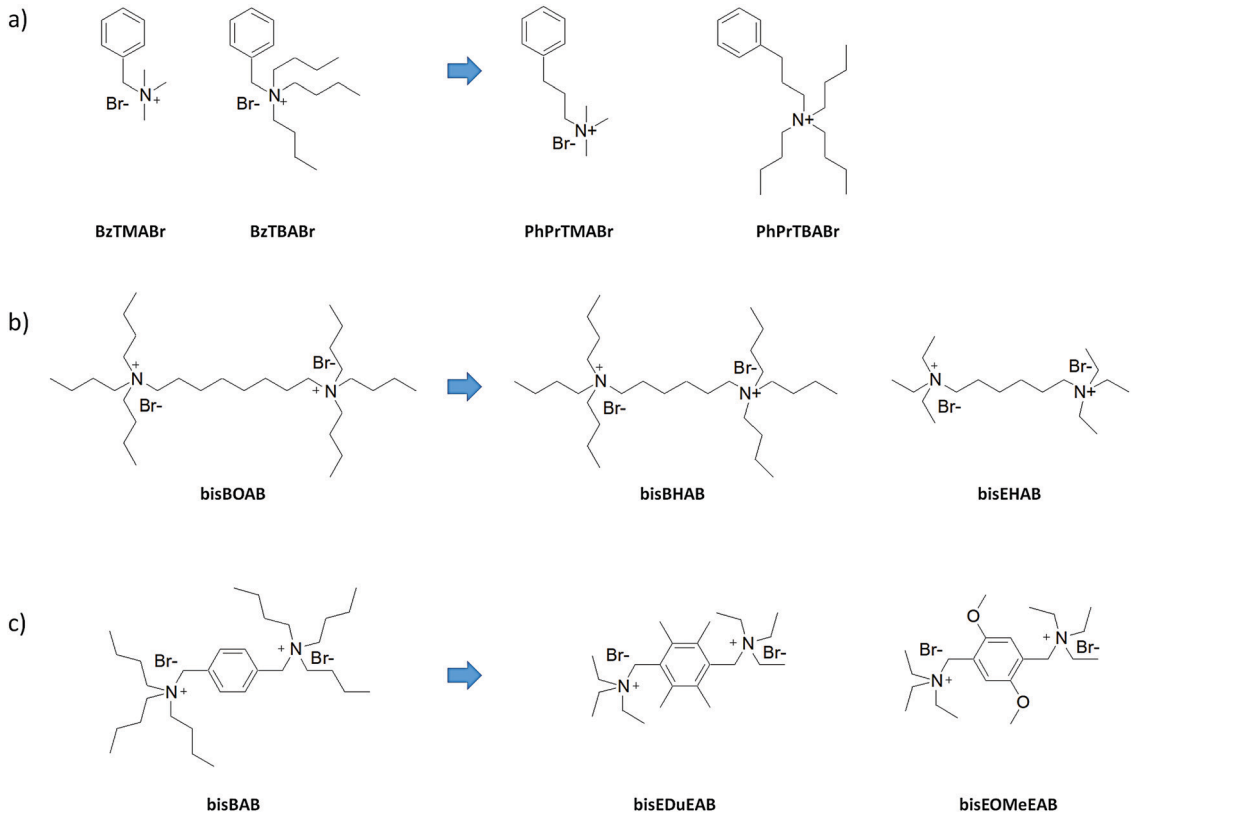

Fig. 1 Design of new ammonium additives. Previously tested compounds are shown on the left, while designed structures are illustrated on the right. (a) aromatic substituted quaternary ammonium additives; (b) diammonium-based additives with a flexible linker; and (c) diammonium-based additives with a rigid linker.

modeling suggested the interaction of the phenyl ring with W215 and the orientation of the tributylammonium moiety towards the catalytic triad as key factors in superactivation. Therefore, we used the interaction model to evaluate whether a longer linker between the ammonium and the phenyl moiety could be favorable or detrimental for superactivation to occur. In particular, due to synthetic accessibility, the new additives PhPrTMABr and PhPrTBABr were designed and their most probable binding poses and similarity scores were compared to corresponding BzTMABr and BzTBABr (Fig. 2).

Our model suggested that the presence of a propane linker still allows the ammonium moiety of the additive to interact with the hydrophobic moiety corresponding to H57 close to the catalytic triad. In the case of the trimethylammonium head groups (Fig. 2a and b) the propane linker seems to facilitate such interaction, increasing the percentage of poses oriented towards the triad. However, compared to the benzyl analogues, PhPrTMABr and PhPrTBABr are located much closer to the catalytic site. Therefore, we decided to synthesize PhPrTMABr and PhPrTBABr, which were predicted to be α-CT superactivators, but the extent of superactivation was uncertain, due to the location of the ammonium group that resulted very close to the catalytic site.

Thus, PhPrTMABr and PhPrTBABr were synthesized and their effect on α-CT activity was studied to compare the new results with those obtained for BzTMABr and BzTBABr. Fig. 3 illustrates the behavior of the ratio between the reaction rate in the additive solution and in pure buffer (r_{add}/r_b) as a function of the additive concentration for PhPrTMABr and PhPrTBABr.

As predicted by the *in silico* design, both additives produced an activating effect on the enzyme, and a bell-shaped trend was observed as the concentration of the additive increased; the maximum of activity was recorded at 0.1 M for both additives. Comparing these results with those previously obtained with the benzyl analogues, however, it was observed that the presence of a propane linker produced a notable decrease in superactivity, almost 40% (from 4.7 to 2.9) for the trimethyl derivative and more than 50% (from 12.4 to 5.4) for the tributyl one. Moreover, the positive effect of a bulky and hydrophobic ammonium group was less evident compared to benzyl additives. Kinetic parameters were determined to deeply understand the effect of these novel additives on enzyme activity and the cause of their lower superactivation with respect to BzTMABr and BzTBABr. Table 1 reports enzyme-substrate affinity (Michaelis constant, K_M), turnover number (k_{cat}), ratio between k_{cat} values in the presence of additive and in pure buffer ($k_{cat(add)}/k_{cat(b)}$) and k_{cat}/K_M values. Experiments were performed at the additive concentration that produced the maximum superactivation effect.

Enzyme-substrate affinity decreased significantly in the presence of the two additives but, at the same time, an increase of turnover number than in pure buffer was also found. These trends were very similar to those observed with the benzyl analogues. As regards k_{cat}, trimethylammonium-based derivatives

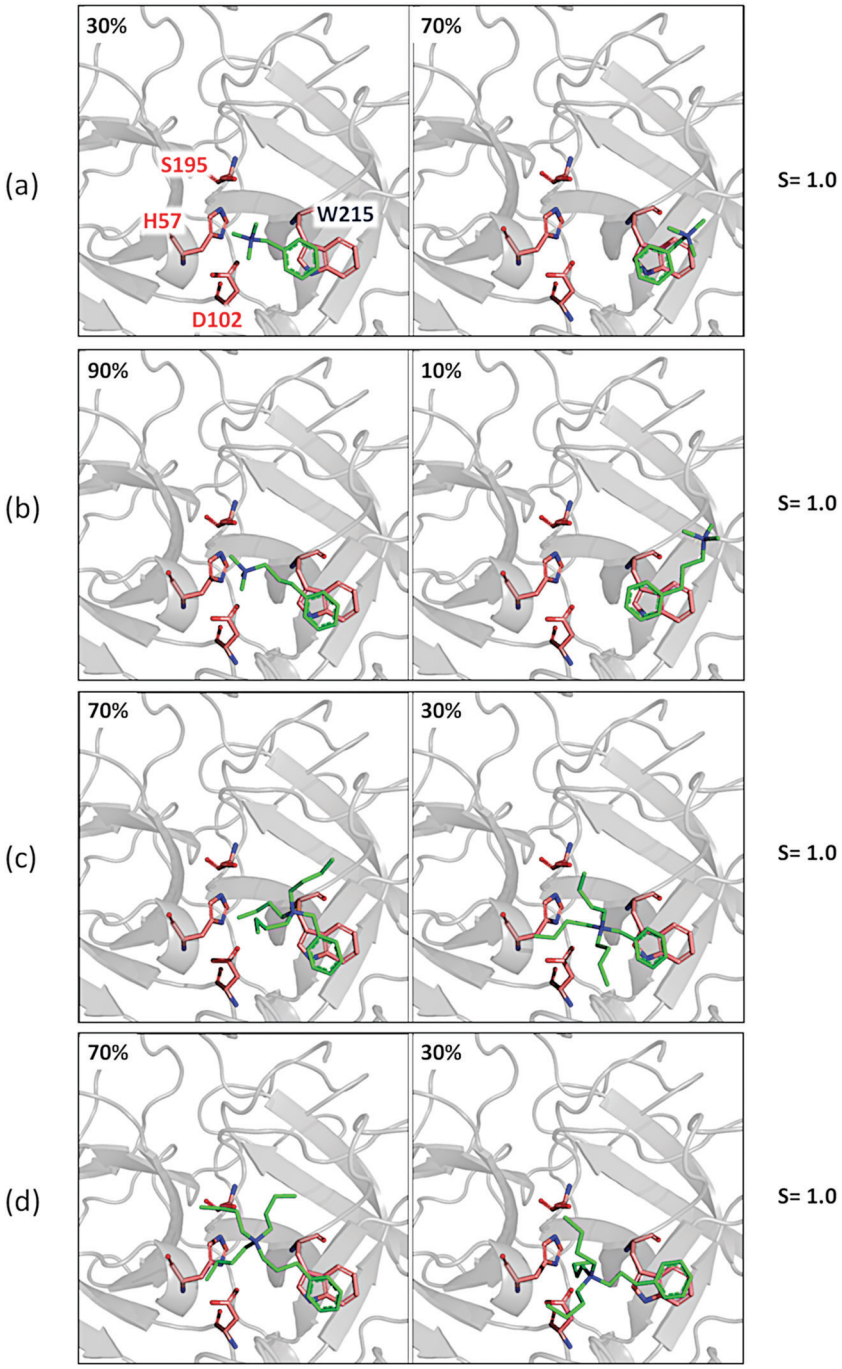

Fig. 2 Most probable binding poses for BzTMABr (a), PhPrTMABr (b), BzTBABr (c) and PhPrTBABr (d). For each additive, the ten top-ranked binding poses were analyzed and clustered in the two most different poses, associated with a percentage of occurrence. The similarity score *S* calculated according to the Glob-Prod descriptor of FLAP is provided (S195: serine 195; H57: histidine 57; W215: tryptophan 215; D102: aspartate 102).

showed similar values, while a decrease of only 20% was observed from BzTBABr to PhPrTBABr. In summary, the lower superactivation produced by the new additives was mainly due to the enhancement in K_M, which was much more pronounced. In particular, the increase in K_M in the presence of BzTMABr and BzTBABr was of about 3- and 4.5-fold with respect to the buffer, respectively, while for PhPrTMABr and PhPrTBABr it was 8.4- and 11-fold higher than in the buffer. A possible explanation for this increase in the K_M values for PhPrTMABr and PhPrTBABr is that, when a propane linker is used, the access of the substrate to the catalytic cavity is partially hampered reducing the enzyme–substrate affinity. Alternatively, the additive may interact with GPNA making the interaction between enzyme and substrate less efficient.

A crystal structure of the GPNA/α-CT complex is not available so far. Thus, the FLAP software was used to predict the most

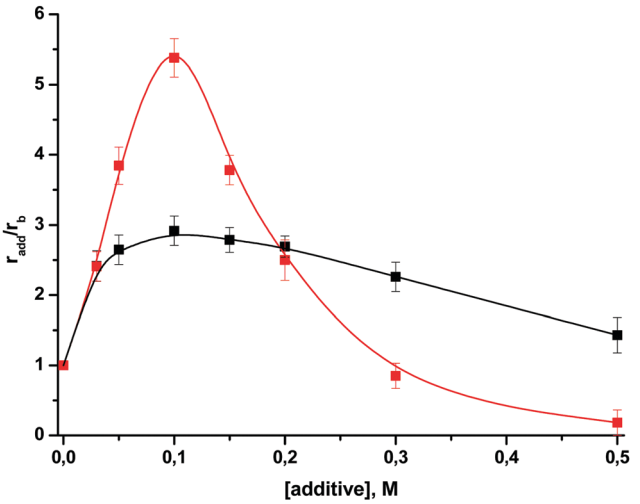

Fig. 3 Effect of PhPrTMABr (black) and PhPrTBABr (red) concentration on the activity of α-chymotrypsin in 0.1 M Tris–HCl buffer, pH 7.75 at 25.0 °C.

Table 1 α-Chymotrypsin kinetic parameters in the presence and absence of additives in 0.1 M Tris–HCl buffer (pH 7.75) at 25.0 °C

Additive	K_M, mM	$10^2 k_{cat}$, s^{-1}	$k_{cat(add)}/k_{cat(b)}$	k_{cat}/K_M, M^{-1} s^{-1}
—	0.44	1.46	—	33.2
BzTMABr 0.4 M[a]	1.37	8.70	5.96	63.5
PhPrTMABr 0.1 M	3.71	10.27	7.03	27.7
BzTBABr 0.15 M[a]	1.99	31.10	21.30	156.3
PhPrTBABr 0.1 M	5.00	24.80	17.00	49.6

[a] From ref. 21.

probable binding mode of GPNA. Two most probable poses were found (Fig. S1 in ESI†), in which only one was a potentially reactive pose (Fig. S1-a, ESI†), with the corresponding mechanism of hydrolysis depicted in Fig. S2 (ESI†). Indeed, it is well-known that several binding modes are commonly associated with a substrate, but only a few poses generally are compatible with a reactive event catalyzed by the enzyme. Once the most probable reactive pose for GPNA is determined, this pose was visualized in the α-CT cavity together with PhPrTMABr, PhPrTBABr, BzTMABr and BzTBABr (Fig. 4).

Fig. 4 is not a real simulation of the interaction of the three molecules (enzyme, additive and substrate), as the substrate and the additive were docked into the protein cavity independently of each other. However, considering that the additive is added to the enzyme buffered solution before the substrate, Fig. 4 suggests that, while BzTBABr and BzTMABr are positioned well at the bottom of the region of interaction of the substrate, simply defining its bottom edge (Fig. 4a and b, respectively), PhPrTBABr and PhPrTMABr are localized much close to the substrate (Fig. 4c and d, respectively). In particular, PhPrTBABr partially occupies the substrate region, and indeed this additive is associated with the highest K_M value in the series (Table 1). In the case of PhPrTMABr, the reduced size of the head group does not induce an overlap of the poses for the additive and the substrate; however, the *N*-trimethyl moiety of PhPrTMABr is very close to the carboxylic function of GPNA,

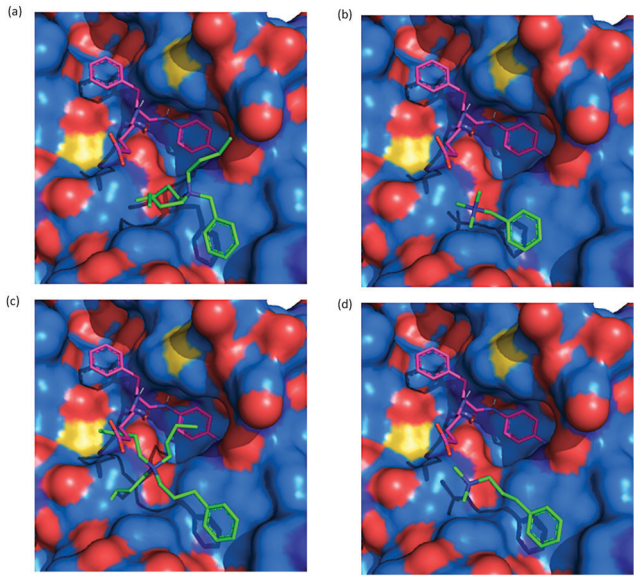

Fig. 4 Simultaneous visualization of GPNA and the additives docked into the α-CT cavity. GPNA is shown in purple. The most probable binding pose for BzTBABr (a), BzTMABr (b), PhPrTBABr (c), and PhPrTMABr (d).

suggesting a potential electrostatic interaction that could perturb the orientation of the substrate into the catalytic cavity (Fig. 4-d and Fig. S3, ESI†).

3.3 Diammonium additives with flexible linker and their effect on α-CT activity

Concerning the diammonium additives with a flexible linker (Fig. 1-b), the superactivation effect of bisBOAB, was found to be lower than the one observed for BzTBABr, and we previously hypothesized that this could be related to the greater flexibility. Thus, the design aimed at verifying the most probable binding modes for two analogues of bisBOAB, having a hexane linker with a triethyl moiety (bisEHAB) or a tributyl moiety (bisBHAB), to modulate hydrophobicity and/or flexibility.

The most probable binding poses for bisBOAB and its analogues are shown in Fig. 5.

The analysis of the binding poses indicated that the shortening of the linker still allows one tributyl-ammonium based derivative to anchor W215 and orients the other towards the catalytic cavity where substrate is usually located (Fig. 5a and b). In particular, the most probable pose for bisBOAB (Fig. 5-a, right panel) is actually very similar to the most probable one for bisBHAB (Fig. 5-b, left panel), as bisBOAB makes a c-curve with the linker that results spatially very similar to the C6-length. Concerning bisEHAB, however, the reduced hindrance at the ammonium level and the shorter linker makes the binding poses much more variable (Fig. 5-c), suggesting a lower catalytic effect.

Fig. 6 shows the activity profile of α-CT in the presence of buffered solutions of newly synthesized bisEHAB and bisBHAB at varying concentrations.

The two observed trends were rather different. Indeed, in the presence of bisEHAB, the relative rate increased by just a factor of 2 and then remained almost constant in a wider

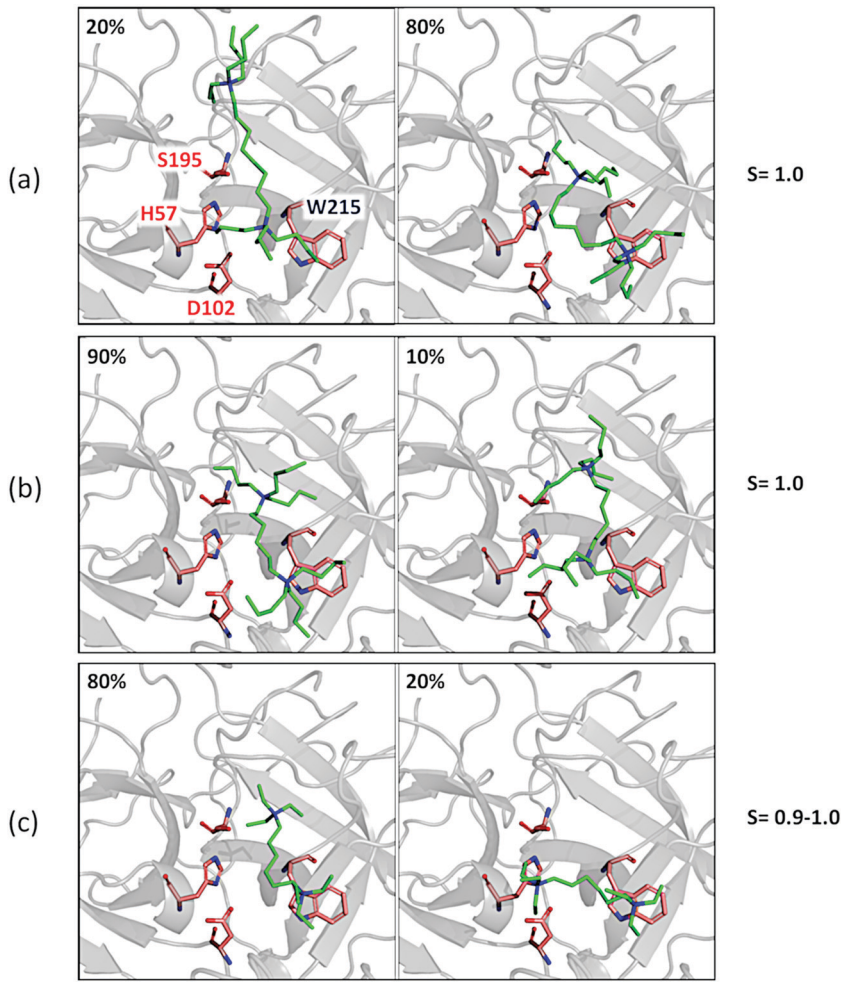

Fig. 5 The most probable binding poses for bisBOAB (a), bisBHAB (b), bisEHAB (c). For each additive, the ten top-ranked binding poses were analyzed and clustered in the two most different poses, associated with a percentage of occurrence. The similarity score *S* calculated according to the Glob-Prod descriptor of FLAP is provided.

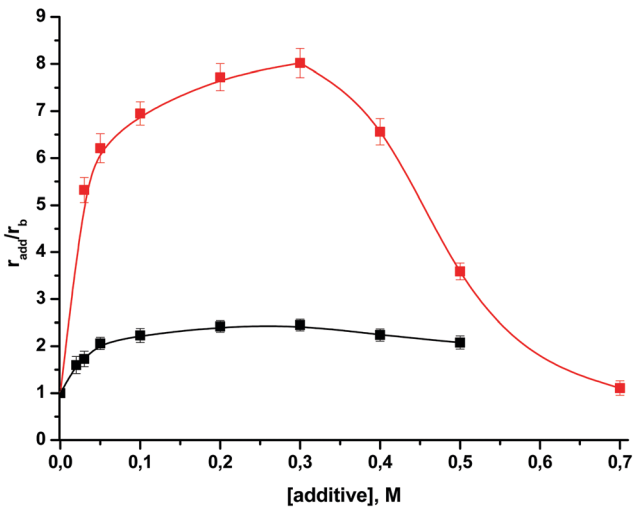

Fig. 6 Effect of bisEHAB (black) and bisBHAB (red) concentration on the activity of α-chymotrypsin in 0.1 M Tris–HCl buffer, pH 7.75 at 25.0 °C.

concentration range. On the other hand, a bell-shaped trend of activity was obtained by varying bisBHAB concentration with a maximum activity observed at 0.3 M, in which enzyme superactivation was about 8-fold compared to that of pure buffer. This behavior was similar to that previously obtained with 0.4 M TBABr and 0.1 M bisBOAB.[21] The presence of the three additives, in fact, increased the rate of the hydrolysis reaction by about 8-fold, confirming once again the essential role played by the tributyl head group.

As previously described,[21] a comparison of the kinetic parameters of TBABr with bisBOAB indicated that, despite a similar superactivation, the addition of bisBOAB increased the enzyme–substrate affinity, but also decreased the k_{cat} value. Thus, the effects of bisEHAB and bisBHAB on enzyme kinetic parameters were also determined and results are shown in Table 2.

As would be expected, in bisEHAB solutions the two-fold activation with respect to buffer was essentially due to an increase in k_{cat} value, with K_M value that increased of about 70%. The effect of bisBHAB on both enzyme–substrate affinity and turnover number was very similar to that observed in

Table 2 α-Chymotrypsin kinetic parameters in the presence and absence of additives in 0.1 M Tris–HCl buffer (pH 7.75) at 25.0 °C

Additive	K_M, mM	$10^2 k_{cat}$, s^{-1}	$k_{cat(add)}/k_{cat(b)}$	k_{cat}/K_M, M^{-1} s^{-1}
—	0.44	1.46	—	33.2
bisEHAB 0.3 M	0.70	3.28	2.25	46.9
bisBOAB 0.1 M[a]	1.86	19.29	13.21	103.8
bisBHAB 0.3 M	1.96	18.44	12.63	94.1

[a] From ref. 21.

bisBOAB, despite the increase in the concentration required to achieve the same superactivation. This result seemed to confirm the outcomes of modeling studies, according to which the linker length did not significantly change the binding poses of the two additives and therefore their effect on α-CT performance.

3.4 Diammonium additives with a rigid linker and their effect on α-CT activity

Concerning the diammonium additives with a rigid linker (Fig. 1-c), we aimed at investigating the effect of substituents in the aromatic moiety. Therefore, having bisBAB as reference compounds, a first *in silico* study was performed to evaluate the binding poses for analogue additives bisEDuBAB and bisEOMeBAB, bearing a durene or a 1,4-dimethoxybenzene scaffold instead of the dibenzyl moiety respectively (Fig. S4 in ESI†). According to our model, the replacement of four aromatic hydrogens with methyl groups in bisEDuBAB led to a similarity score, which was identical to that of BisBAB (S = 1), and very similar poses as well. Both for bisBAB and bisEDuBAB, a tributylammonium moiety was involved in the interaction with W215, with the additive displaying two different orientations in the cavity. However, for bisEDuBAB the pose having the aromatic moiety located closer to the catalytic site resulted in being more favored (Fig. S4-a and b in ESI†). When polar substituents are added to the bisBAB scaffold, molecular modelling studies indicated that a totally different binding mode is preferred. In addition, the similarity score for bisEOMeBAB was lower than the ones for bisBAB and bisEDuBAB, suggesting a less efficient interaction with the protein. The reduced similarity score seems to be mainly related to the lack of

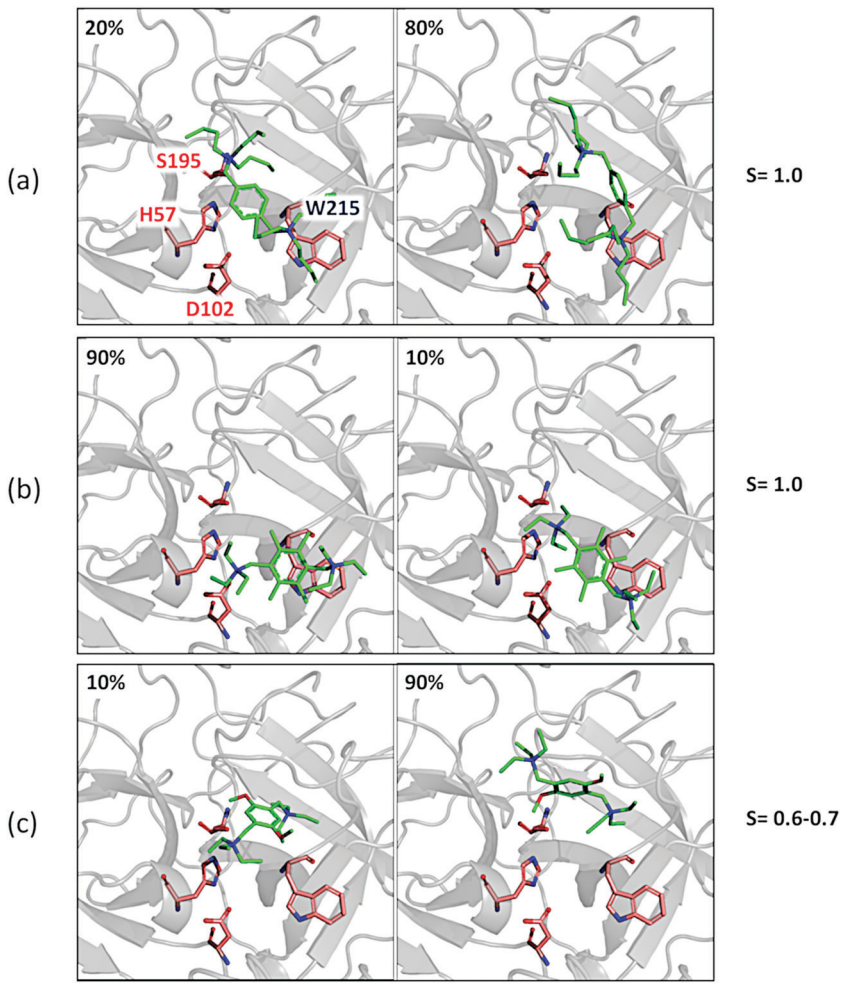

Fig. 7 The most probable binding poses for bisBAB (a), bisEDuEAB (b) and bisEOMeEAB (c). For each additive, the ten top-ranked binding poses were analyzed and clustered in the two most different poses, associated with a percentage of occurrence. The similarity score S calculated according to the Glob-Prod descriptor of FLAP is provided.

interaction with W215, which induces bisEOMeBAB to move towards the inner part of the cavity competing with GPNA (Fig. S4-c and S5 in ESI†).

Unfortunately, synthetic accessibility and solubility issues hampered the investigation of bisEDuBAB and bisEOMeBAB; thus, the triethyl analogues bisEDuEAB and bisEOMeEAB were synthesized and tested instead. Fig. 7 shows the FLAP most probable binding poses for the two tested compounds, and the poses for bisBAB are also provided for reference.

For bisEDuEAB a similarity score of 1 was obtained, as for bisBAB and bisEDuBAB (S = 1). Nevertheless, the hypothesized binding modes were rather different, with bisEDuEAB being not able to reach the oxyanion hole region. This effect seems to be due, not to the substituents but to the triethyl ammonium head group, as suggested by comparison with the bisEDuBAB binding poses. Concerning bisEOMeEAB, the similarity score was even lower than that for the tributyl analogue and again lower than the ones for bisBAB and bisEDuAEB, suggesting a less efficient interaction with the protein depending not only on the substitution with polar groups but also on the head group size. As for bisEOMeBAB, an interaction with W215 was not observed.

Based on these considerations, a lower catalytic effect was expected for bisEDuEAB and bisEOMeEAB compared to bisBAB. Fig. 8 reports the activity profile of α-CT in the presence of bisEOMeEAB and bisEDuEAB as a function of additive concentration.

Results obtained with the two diammonium additives having a rigid linker were quite different from each other and compared with bisBAB, the reference additive previously studied.[21] Both curves of reaction rate *versus* surfactant concentration were bell-shaped, with a maximum of activity at an additive concentration of 0.1 M and 0.05 M for bisEOMeEAB and bisEDuEAB, respectively. However, superactivation effect produced by the most hydrophobic additive, bisEDuEAB (about 15-fold), not only was higher than bisEOMeEAB (4.5-fold) and bisBAB (6-fold), but it was the highest ever obtained with cationic additives, both surfactants and salts, studied so far. In this case, the hydrophobicity was not due to the bulky tributyl head groups, but to the hydrophobic substituents linked to the aromatic ring. Simultaneous visualization of GPNA and bisEDuEAB docked into the α-CT cavity is shown in the ESI† (Fig. S6). On the other hand, the presence of two methoxy groups, capable of forming hydrogen bonds, probably made the catalytic site much more polar, with a consequent decrease in enzymatic superactivity.

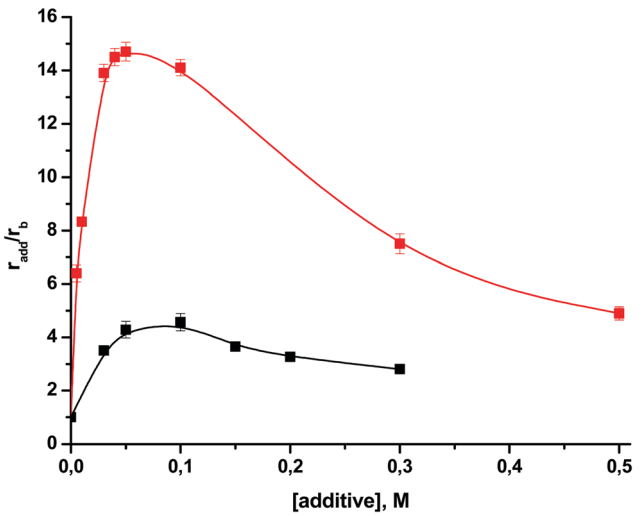

Fig. 8 Effect of bisEOMeBAB (■) and bisEDuEAB (■) concentration on the activity of α-chymotrypsin in 0.1 M Tris–HCl buffer, pH 7.75 at 25.0 °C.

Table 3 α-Chymotrypsin kinetic parameters in the presence and absence of additives in 0.1 M Tris–HCl buffer (pH 7.75) at 25.0 °C

Additive	K_M, mM	$10^2 k_{cat}$, s^{-1}	$k_{cat(add)}/k_{cat(b)}$	k_{cat}/K_M
—	0.44	1.46	—	33.2
bisBAB 0.1 M[a]	1.49	12.00	8.20	80.5
bisEDuEAB 0.05 M	0.96	24.80	16.99	258.3
bisEOMeEAB 0.1 M	0.96	6.59	4.51	68.6

[a] From ref. 21.

Kinetic parameters were also determined and results are provided in Table 3.

Enzyme-substrate affinity for both additives was lower than buffer, K_M being double compared to the reference, but was less than other superactivating additives, which for BzTBABr and bisBOAB was about 2 mM and for cetyltributylammonium bromide (CTBABr)[16] and tetrabutylammonium bromide (TBABr)[18] were 3.7 mM and 6.1 mM, respectively.

An increase in k_{cat} was observed for both additives, but their effects were very different, *i.e.* 4.5-fold for bisEOMeEAB and 17-fold for bisEDuEAB.

The value of the turnover number obtained with bisEDuEAB was not the highest reached, since in the presence of BzTBABr and TBABr, it was equal to 31 × 10^2 s^{-1} but, given the greater affinity of the enzyme for the substrate, the catalytic efficiency was certainly the highest reached until now.

These results seemed to confirm once again the key role of hydrophobic moieties on the structure of the additive in the superactivation of α-CT, which can increase the nucleophilicity of the catalytic serine. On the other hand, however, one or more bulky head groups hinder the access of the substrate into the active site, slightly reducing the superactivity.

4. Conclusions

In this research work, an *in silico* model previously used to rationalize kinetic behaviors and superactivation effects of a few quaternary ammonium salts toward α-CT was applied to design new ammonium-based additives of three different chemical series, with the double aim of testing the predicting capabilities of the model and to get new insights into the key interaction in α-CT superactivation. The *in silico* prediction well correlated with experimental findings not only based on the similarity scores obtained, but especially when a binding mode analysis is performed.

Regarding phenyl-based additives, the significant reduction in enzyme superactivity observed when a propane linker replaced a methylene was due to an increase in K_M, and molecular modelling studies suggested that these additives partially occupy the substrate interaction region, hindering its access to the active site. The hydrophobic interaction resulted in being critical to improve superactivation, and this was especially evident for the series of diammonium additives bearing a rigid linker. Indeed, bisEDuEAB, which was designed, synthesized and tested in this study, is the most effective ammonium additive studied so far. In addition, bisEDuEAB contrasts the paradigm that bulky hydrophobic head groups are needed to increase the superactivation effect, since the overall hydrophobicity seems to play a role. The presence of hydrophobic substituents linked to the aromatic ring instead of to the head group produced a more hydrophobic microenvironment with a consequent increase in the nucleophilicity of the catalytic serine residue and also allowed an easier entry of the substrate into the active site (lower K_M value than tributyl additives). The amino acid W215 was confirmed to be a key residue for interaction with superactivating additives. Finally, kinetic parameters were interpreted for the first time also taking into account the potential binding mode of the substrate.

Conflicts of interest

There are no conflicts of interest to declare.

Acknowledgements

The authors acknowledge the financial support by the University of Perugia (Fondo Ricerca di Base 2019).

References

1 D. G. Herries, Enzyme Structure and Mechanism (Second Edition), *Biochem. Educ.*, 1985, **13**(3), 146.
2 D. M. Blow, *The Structure of Chymotrypsin*, 1971, **3**, 185–2126.
3 G. P. Hess, in *The Enzymes*, ed. B. P. D., Academic Press, New York, 3rd edn, 1971, vol. 3, pp. 213–248.
4 S. K. Verma and K. K. Ghosh, Effect of cationic surfactants on the enzymatic activity of α-chymotrypsin, *Kinet. Catal.*, 2011, **52**(1), 6–10.
5 M. S. Celej, M. G. D'Andrea, P. T. Campana, G. D. Fidelio and M. L. Bianconi, Superactivity and conformational changes on alpha-chymotrypsin upon interfacial binding to cationic micelles, *Biochem. J.*, 2004, **378**(3), 1059–1066.
6 E. Abuin, E. Lissi and C. Calderón, Kinetics of *N*-glutaryl-l-phenylalanine *p*-nitroanilide hydrolysis catalyzed by α-chymotrypsin in aqueous solutions of alkyltrimethylammonium bromides, *J. Colloid Interface Sci.*, 2007, **308**(2), 573–576.
7 S. K. Verma, B. K. Ghritlahre, K. K. Ghosh, R. Verma, S. Verma and X. Zhao, Influence of Amine-Based Cationic Gemini Surfactants on Catalytic Activity of α-Chymotrypsin, *Int. J. Chem. Kinet.*, 2016, **48**(12), 779–784.
8 Y. A. Valiullina, E. A. Ermakova, D. A. Faizullin, A. B. Mirgorodskaya and Y. F. Zuev, Structure and catalytic activity of α-chymotrypsin in solutions of gemini surfactants, *Russ. Chem. Bull.*, 2014, **63**(1), 273–279.
9 G.-Y. Bai, J.-L. Liu, J.-X. Wang, Y.-J. Wang, Y.-N. Li, Y. Zhao and M.-H. Yao, Enzymatic Superactivity and Conformational Change of α-CT Induced by Cationic Gemini Surfactant, *Acta Phys.-Chim. Sin.*, 2017, **33**(5), 976–983.
10 T. Kurinomaru, T. Kameda and K. Shiraki, Effects of multivalency and hydrophobicity of polyamines on enzyme hyperactivation of α-chymotrypsin, *J. Mol. Catal. B: Enzym.*, 2015, **115**, 135–139.
11 A. Endo, T. Kurinomaru and K. Shiraki, Hyperactivation of α-chymotrypsin by the Hofmeister effect, *J. Mol. Catal. B: Enzym.*, 2016, **133**, S432–S438.
12 A. Endo, T. Kurinomaru and K. Shiraki, Hyperactivation of serine proteases by the Hofmeister effect, *Mol. Catal.*, 2018, **455**, 32–37.
13 A. Wangler, R. Canales, C. Held, T. Q. Luong, R. Winter, D. H. Zaitsau, S. P. Verevkin and G. Sadowski, Co-solvent effects on reaction rate and reaction equilibrium of an enzymatic peptide hydrolysis, *Phys. Chem. Chem. Phys.*, 2018, **20**(16), 11317–11326.
14 C. Held, T. Stolzke, M. Knierbein, M. W. Jaworek, T. Q. Luong, R. Winter and G. Sadowski, Cosolvent and pressure effects on enzyme-catalysed hydrolysis reactions, *Biophys. Chem.*, 2019, **252**, 106209.
15 M. Knierbein, C. Held and G. Sadowski, The role of molecular interactions on Michaelis constants of α-chymotrypsin catalyzed peptide hydrolyses, *J. Chem. Thermodyn.*, 2020, **148**, 106142.
16 N. Spreti, F. Alfani, M. Cantarella, F. D'Amico, R. Germani and G. Savelli, α-Chymotrypsin superactivity in aqueous solutions of cationic surfactants, *J. Mol. Catal. B: Enzym.*, 1999, **6**(1-2), 99–110.
17 F. Alfani, M. Cantarella, N. Spreti, R. Germani and G. Savelli, α-Chymotrypsin Superactivity in Cetyltrialkylammonium Bromide-Rich Media, *Appl. Biochem. Biotechnol.*, 2000, **88**(1-3), 001–016.
18 N. Spreti, P. Di Profio, L. Marte, S. Bufali, L. Brinchi and G. Savelli, Activation and stabilization of α-chymotrypsin by cationic additives, *Eur. J. Biochem.*, 2001, **268**(24), 6491–6497.
19 F. De Angelis, A. Di Tullio, P. Del Boccio, S. Reale, G. Savelli and N. Spreti, ESI-MS in the study of the activity of α-chymotrypsin in aqueous surfactant media, *Org. Biomol. Chem.*, 2003, **1**(17), 3125–3130.
20 N. Spreti, M. V. Mancini, R. Germani, P. Di Profio and G. Savelli, Substrate effect on α-chymotrypsin activity in aqueous solutions of ''big-head'' ammonium salts, *J. Mol. Catal. B: Enzym.*, 2008, **50**(1), 1–6.
21 L. De Matteis, F. Di Renzo, R. Germani, L. Goracci, N. Spreti and M. Tiecco, α-Chymotrypsin superactivity in quaternary ammonium salt solution: kinetic and computational studies, *RSC Adv.*, 2016, **6**(52), 46202–46211.
22 J. Weinstock, Anomalous Hofmann Elimination Reactions, *J. Org. Chem.*, 1956, **21**, 540–542.

23 H. J. Barber and K. Gaimster, Hexamethonium Bitartrate and Other Hexa-Alkonium Salts, *J. Pharm. Pharmacol.*, 1951, **3**(1), 663–669.
24 T. Iwaguchi, Supporting Electrolyte of Polarography, *Yakugaku Zasshi*, 1961, **81**(6), 925–927.
25 L. Brinchi, R. Germani, L. Goracci, G. Savelli and C. A. Bunton, Decarboxylation and Dephosphorylation in New Gemini Surfactants. Changes in Aggregate Structures, *Langmuir*, 2002, **18**(21), 7821–7825.
26 N. N. P. Mel'nikov and M. V. Prilutskaya, Chloromethylation of ethers of bivalent phenols and some of their transformations, *Zh. Obshch. Khim.*, 1959, **29**, 3746–3752.
27 M. Baroni, G. Cruciani, S. Sciabola, F. Perruccio and J. S. Mason, A Common Reference Framework for Analyzing/Comparing Proteins and Ligands. Fingerprints for Ligands And Proteins (FLAP): Theory and Application, *J. Chem. Inf. Model.*, 2007, **47**(2), 279–294.
28 P. J. Goodford, A computational procedure for determining energetically favorable binding sites on biologically important macromolecules, *J. Med. Chem.*, 1985, **28**(7), 849–857.
29 E. Carosati, S. Sciabola and G. Cruciani, Hydrogen Bonding Interactions of Covalently Bonded Fluorine Atoms: From Crystallographic Data to a New Angular Function in the GRID Force Field, *J. Med. Chem.*, 2004, **47**(21), 5114–5125.
30 G. Muratore, L. Goracci, B. Mercorelli, A. Foeglein, P. Digard, G. Cruciani, G. Palu and A. Loregian, Small molecule inhibitors of influenza A and B viruses that act by disrupting subunit interactions of the viral polymerase, *Proc. Natl. Acad. Sci. U. S. A.*, 2012, **109**(16), 6247–6252.
31 S. Massari, G. Nannetti, L. Goracci, L. Sancineto, G. Muratore, S. Sabatini, G. Manfroni, B. Mercorelli, V. Cecchetti, M. Facchini, G. Palù, G. Cruciani, A. Loregian and O. Tabarrini, Structural Investigation of Cycloheptathiophene-3-carboxamide Derivatives Targeting Influenza Virus Polymerase Assembly, *J. Med. Chem.*, 2013, **56**(24), 10118–10131.
32 C. G. Fortuna, C. Bonaccorso, A. Bulbarelli, G. Caltabiano, L. Rizzi, L. Goracci, G. Musumarra, A. Pace, A. Palumbo Piccionello, A. Guarcello, P. Pierro, C. E. A. Cocuzza and R. Musumeci, New linezolid-like 1,2,4-oxadiazoles active against Gram-positive multiresistant pathogens, *Eur.* J, *Med. Chem.*, 2013, **65**, 533–545.